Antibacterial Properties of Cu - ZrO_2 Thin Film Prepared *via* Aerosol Assisted Chemical Vapour Deposition

Abdullah M. Alotaibi[a], Sanjayan Sathasivam[a,b], Sean P. Nair[c] and Ivan P. Parkin[a]*

*Corresponding author

[a]Materials Chemistry Centre, Department of Chemistry, University College London, 20 Gordon Street, London WC1H 0AJ, UK

Fax: (+44) 20-7679-7463

E-mail: i.p.parkin@ucl.ac.uk

[b]Bio Nano Consulting Ltd, The Gridiron Building, One St. Pancras Square, London N1C 4AG, UK

Fax: (+44) 20-7396-1056

E-mail: info@bio-nano-consulting.com

[c]Department of Microbial Diseases, University College London Eastman Dental Institute, 256 Gray's Inn Road, London, WC1X 8LD, UK

Abstract

The antibacterial properties of a Cu – ZrO_2 film grown *via* aerosol assisted chemical vapour deposition are presented. The composite film showed high activity against *E. coli* (Gram-negative) and *S. aureus* (Gram-positive) bacteria with 5 $\log_{10}$ (*E. coli*) and 4 $\log_{10}$ (*S. aureus*) decrease in viable bacteria achieved within 20 and 60 minutes respectively. These results were comparable to a pure copper film that was prepared under the same conditions. The composite film was characterized for material properties using a range of techniques including X-ray photoemission and X-ray diffraction.

Introduction

Hospital acquired infections (HAI) are a leading heath care problem affecting millions of patients every year.[1,2] Infections caused by multidrug resist strains of bacteria due to decades of inappropriate antibiotic use are of particular concern. [3,4] HAI in majority of cases are caused by spread of bacteria through contact with contaminated surfaces in health care environments and as such alternative approaches to disinfection are key to reduction of infections.

Antimicrobial coatings consisting of metals (Cu or Ag), metal oxides (TiO_2 or ZnO) and even organic compounds (methylene blue) encased in polymers have the potential to provide highly effective unorthodox routes to creating active decontamination surfaces.[5] Applying these coatings to high contact 'touch surfaces' (door handles and computer keyboards) found in hygiene sensitive environments has been shown to reduce microbial contamination.[6-8]

Antimicrobial coatings also play an important role in minimizing infections of orthopedic and dental implants that are the main cause of implant complications and failure.[9, 10] The primary reasons for infection of the implant surface are the formation of a protein layer, which helps with biocompatibility but also allows bacteria to colonise and compromised host immunity ability at the implant-tissue interface.[9, 11] Antimicrobial coatings applied to the implants, which border the junction between the implant and tissue, have been shown to reduce infection.[10] Common applications include antibiotic release from polymer coatings as well as anti-infective silver releasing coatings.[12, 13] Surface modifications of implants using copper and silver have also been studied.[9] Huang et. al showed that titanium, stainless steel and Ti-Al-Nb metal implants had antimicrobial activity against *S. aureus* and increased wear resistance properties compared to pristine samples.[14, 15] Furthermore, Chang and co-workers studied silver and copper doped ZrO_2 coatings on Ti implants and showed that they had increased resistance to colonisation from several types of bacteria.[16]

Copper has a long history of use as an antimicrobial agent to treat wounds and clean water.[17, 18] The mechanism of action is still disputed but one possible method is *via* reactive oxygen species produced through Fenton-type reactions that cause DNA damage.[18, 19] Hence, the use of copper in the form of thin films, powders and nanoparticles powders is well documented in literature. Carmalt and Parkin et al.

found that copper films show good antimicrobial activity against *E. coli* and *S. aureus*.[17] Marikani et at showed that copper nanoparticles produced *via* the reduction of copper acetate hydrate had an antibacterial effect against a range of bacterial including *E. coli, S. aureus and P. aeruginosa.*[20]

Zirconium oxide (ZrO_2) is an important multifunctional material that has been used in fuel cells, gas sensors, catalysis and optical dielectrics and is generally produced *via* sol-gel, hydrothermal and solid-state reactions. Furthermore, it is renowned for its mechanical (high fracture toughness) properties and biocompatibility and research has shown that it can be employed in dental implants or coatings on orthopedic implants such as Ti metal.[16, 21] Since ZrO_2 does not show any intrinsic antimicrobial properties, the formation of composites of ZrO_2 with naturally antimicrobial species such as Cu could be very promising in the fight against bacterial infection of orthopedic and dental implants.[14-16, 21]

In this paper we show for the first time the formation of Cu - ZrO_2 composite films. The motivation being that a composite of Cu-ZrO_2 would be a suitable and convenient coating on orthopedic implants to prevent infection as it enables the facile formation though Aerosol Assisted Chemical Vapour Deposition of a layer with both high biocompatibility and antibacterial properties. The use of AACVD for the formation of the film provides a simple solution based route that is easily scalable.[22, 23] In AACVD the precursors are dissolved in a suitable solvent, atomized and transported into the deposition chamber using a carrier gas.[24] Films produced *via* AACVD are of high quality and have many applications including photovoltaics, optoelectronics and photocatalysis.[25-31] Notably these Cu – ZrO_2 coatings are rugged and very resistant to abrasion.

.

Experimental

General Procedure

Depositions were carried out under nitrogen (99.99% from BOC). Precursors (Copper nitrate hydrate [$Cu(NO_3)_2.3H_2O$] (99%), zirconium acetylacetonate [$Zr(acac)_4$] (99%) and absolute methanol) were placed in a glass bubbler and an aerosol mist was created using a piezoelectric device. All chemicals were procured from Aldrich and were utilised as received.

ZrO_2, Cu and Cu – ZrO_2 thin films were deposited by AACVD. The ZrO_2 film was synthesized using [$Zr(acac)_4$] (1 mmol, 0.48 g) in a methanol solution (40 mL). The Cu film was made from [$Cu(NO_3)_2.3H_2O$] (0.5 mmol, 0.23 g) in methanol and the composite Cu – ZrO_2 film was made from a methanol (40 mL) solution of $Zr(acac)_4$] (1 mmol, 0.48 g) and [$Cu(NO_3)_2.3H_2O$] (0.5 mmol, 0.23 g).

AACVD of the solutions to obtain the corresponding films was carried out on silica (50 nm) coated float glass at 430 °C under N_2 carrier gas at a flow rate of 2 $Lmin^{-1}$ with depositions lasting 45 minutes. Prior to use the glass was washed with water, acetone and isopropanol and allowed to dry in the oven at 100 °C. The cold-walled horizontal-bed CVD reactor contained a carbon block, containing a Whatmann cartridge heater. A Pt–Rh thermocouple was used to control the temperature on the substrate. The reactor has top and bottom plates for deposition and the top plate was placed 8 mm above the substrate. The aerosol mist was generated by a PicoHealth™ ultrasonic humidifier at room temperature.

Film Characterization

XRD data were collected using microfocus Bruker GAADS powder X-ray diffractometer using a monochromated Cu Kα radiation. (XPS) X-ray photoelectron spectroscopy was carried out using a Thermo Scientific K-Alpha instrument with monochromatic Al-K α source. SEM images were carried out on a JEOL 6301F instrument with acceleration voltage of 5 kV. Samples were prepared by cutting to 10 mm × 10 mm and then coated with gold in order to avoid charging. UV-Vis spectroscopy was carried out using both a Lamda 25 and 950 instruments. Water droplet contact angles were carried out using an FTA-1000 drop shape instrument. A Fujifilm Finepix HS25 EXR camera captured image at 1000 frames per second.

Antibacterial Testing

One colony of *Escherichia coli* (ATCC 25922) or *Staphylococcus aureus* (8325-4) was inoculated into 10 mL of brain heart infusion (BHI) (Oxoid, Basingstoke, UK) and incubated with shaking at 200 rpm at 37 °C for 18 hours. The culture was centrifuged at 3000xg for 15 mins to recover the bacteria and washed in phosphate-buffered saline (PBS) (10 ml) (Oxoid, Basingstoke,UK), then centrifuged at 3000×g for 15 minute and re-suspend in 10 ml of (PBS). Finally, suspensions of the bacteria were diluted in 10 ml of phosphate-buffered saline (PBS) to give an inoculum containing approximately 10^6 colony forming units (cfu).

Prior to use, ZrO_2, Cu, Cu-ZrO_2 thin films and uncoated glass controls were cut into (1 × 1 cm) pieces. A humidity chamber was used to prevent drying out of the suspensions. For each exposure time, triplicate samples were analysed with each exposure time being repeated on three separate occasions. A 25 µL aliquot of the bacterial cell suspension was spread evenly on the surface of each sample and incubated at room temperature for the allocated exposure time and covered with coverslips. After incubation the slides were transferred to a 5 mL PBS and vortexed for 40 seconds. Serial dilution of the resulting bacterial suspensions was prepared in PBS and 25 µL from each dilution was spread onto MacConkey agar for E.coli and Mannitol Salt agar (MSA, Oxoid Ltd.) for *S. aureas*. All plates were incubated 24 hours at 37 °C. After incubation, any bacterial colonies were counted and viable counts of bacteria were calculated. The Whitney U test was used to determine the statistical significance of the activity of the ZrO_2, Cu and Cu-ZrO_2 films compared to the uncoated glass control.

Results and Discussion

Thin films of ZrO_2, Cu and a composite Cu – ZrO_2 were produced *via* a simple AACVD method at 430 ^oC. Each deposition was carried out from a one-pot methanol solution of $[Zr(acac)_4]$, $[Cu(NO_3)_2.3H_2O]$ and an mixture of $[Zr(acac)_4]$ and $[Cu(NO_3)_2.3H_2O]$ at two to one molar ratio. All films coated the glass substrate with uniform coverage and were void of pinhole defects and cracks, the films containing ZrO_2 were well adhered to the substrate, passing the Scotch^{TM} tape test (see supporting information). The copper film was noticeably more mechanically weak than the composite film and was readily scratched by a metal spatula. However the composite film resisted scratching and abrasion (see supporting information).

The XRD patterns of the ZrO_2, Cu and Cu – ZrO_2 were carried out to determine the phase purity (Figure 1). ZrO_2 was indexed to the high temperature cubic phase with peaks at 30.3^o, 35.2^o, 50.5^o and 60.3^o 2θ values corresponding to the (111), (200), (220) and (311) reflections respectively. The growth of the cubic phase below 2300 ^oC without the addition of stabilizers is rare but there are literature examples of obtaining this phase at temperatures as low as 400 ^oC, including a CVD route.[32, 33] The Cu film showed the (111) and (200) reflection for metallic copper at 43.3^o and 50.4^o respectively, additionally there were very small peaks at 36.9^o and 62.0^o matching to the (111) and (220) reflections of Cu_2O, a native oxide layer that readily forms on metallic films (see supporting information).[34-38] The composite Cu – ZrO_2 matches peaks corresponding to both cubic ZrO_2 and Cu metal as expected. Further to this, like on the Cu film, close examination of the composite film's XRD pattern shows a peak at 36.9^o matching Cu_2O (111) reflection (see supporting information).[34-38] Again this is due to the partial oxidation of the copper component of the film. This is supported also by XPS analysis (Figure 2).

The Debye – Scherrer formula was applied to the XRD data to compare the crystallite sizes in the ZrO_2, Cu and Cu – ZrO_2 films. The Cu film had the largest crystallite size followed by the Cu phase of the Cu – ZrO_2 composite film. The ZrO_2 component of the composite had the smallest crystallite size (see supporting information).

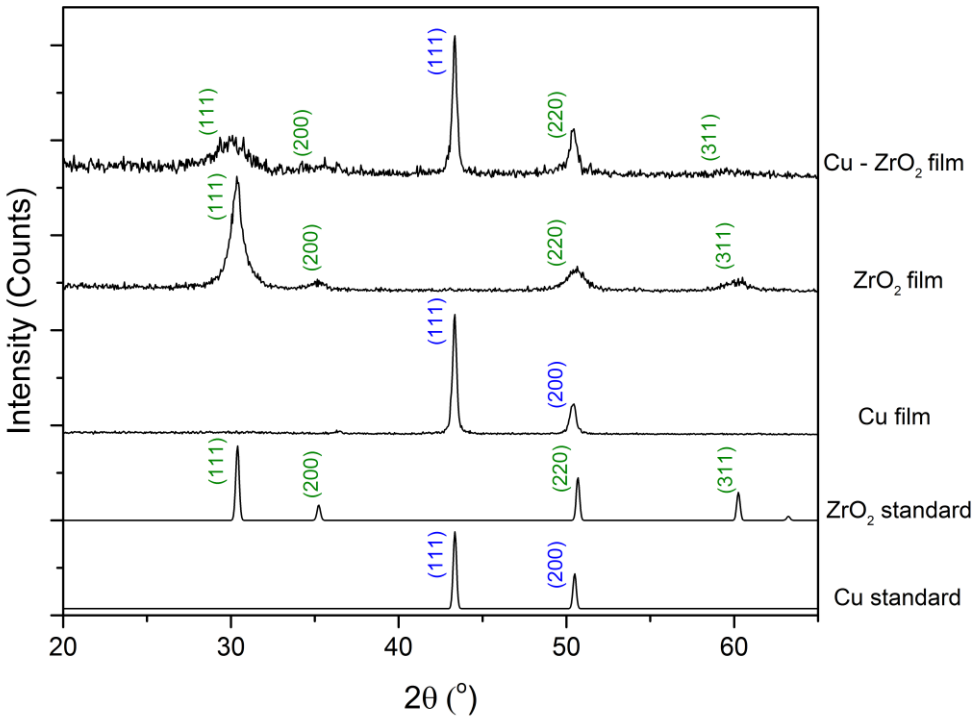

Figure 1: The XRD patterns obtained for the Cu, ZrO_2 and Cu – ZrO_2 composite films grown *via* AACVD. The patterns obtained for the AACVD synthesized films match well with the standard.

Figure 2 shows the X – ray photoemission spectra for the Zr 3d and Cu 2p region for the composite Cu – ZrO_2 film. The $Zr_{5/2}$ peak is centered at 181.9 eV corresponds to Zr in the 4+ oxidation state as expected. Deconvolution of the Cu 2p peak reveals the presence of a mixture of oxidation states. The predominant Cu $2p_{3/2}$ peak centered at 932.5 eV can be assigned to Cu (0) and/or Cu (I) as it is difficult to differentiate between Cu (0) and Cu (I) from the Cu 2p transition alone.[39] But since XRD analysis (see Figure 1) indicates that both Cu metal and a small amount of Cu_2O are present in the composite film it is possible to conclude that both Cu (0) and Cu (I) are present in the XPS spectrum. In addition, there in another peak at 934.6 eV that corresponds to Cu in the 2+ oxidation state.[39, 40] The presence of a Cu (II) species is also supported by the occurrence of the Cu (II) shake-up satellite at 940.3 eV.[39] Elemental analysis of the surface of the film from the sensitivity corrected Zr 3d and Cu 2p peak areas show that the ratio of Cu to Zr was 2.3 to 1 (see supporting information). Also, of the Cu content of the composite film surface, there are 5 times as much Cu (0) / Cu (I) compared to Cu (II) based on the assumption that the contribution to the shake-up satellite peak is solely from the Cu (II) component.[39]

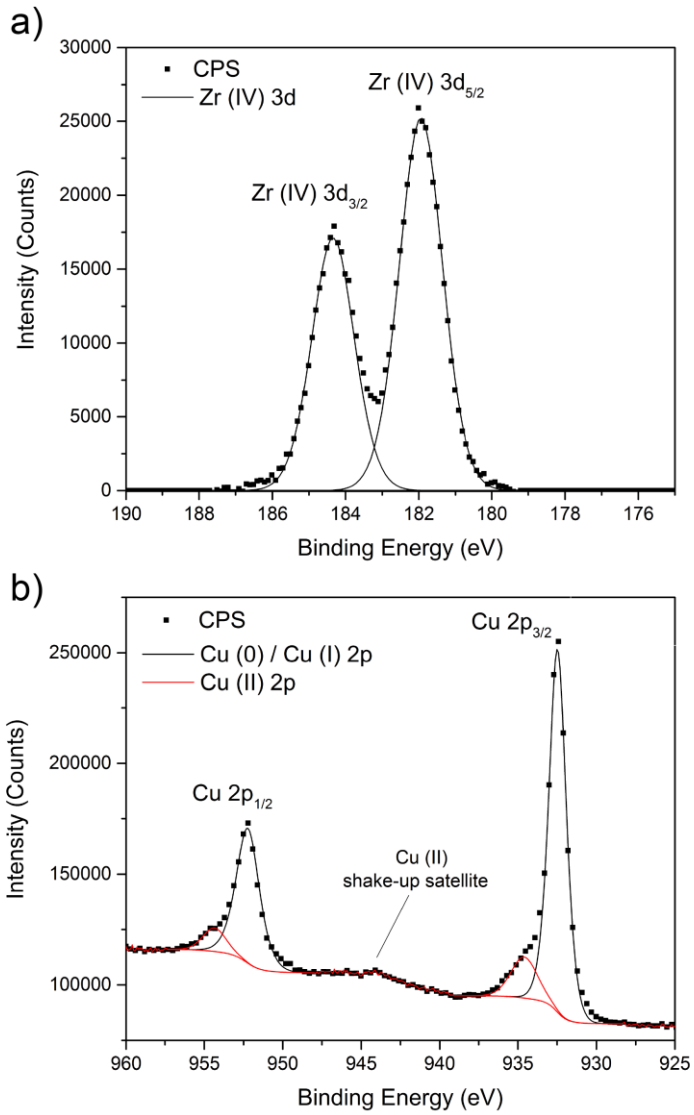

Figure 2: XPS spectra of the Cu – ZrO_2 film showing a) the Zr $3d_{5/2}$ and $3d_{3/2}$ transitions. The Zr $3d_{5/2}$ peak appears at 181.9 eV matching well with literature values for Zr in the 4+ oxidation state. b) Shows the Cu 2p transitions observed for the composite film. The primary peak centered at 932.5 eV matches to Cu metal and Cu in the 1+ oxidation state, an additional minor peak at 934.6 eV and the shake up satellite peak around 943 eV belong to the Cu^{2+} component of the film.

The microstructure of the Cu, ZrO_2 and Cu – ZrO_2 films were probed using electron microscopy (Figure 3). The Cu film showed a morphology made up of particles ranging between 100 – 500 nm in width that were not very densely packed across the areas analysed. The ZrO_2 film also had a similar morphology. The composite Cu - ZrO_2 film however, was made up of densely packed particles roughly 50-75 nm in diameter. This corresponds well with crystallite sizes obtained *via* the Debye-Scherrer equation using XRD data (Figure 1).

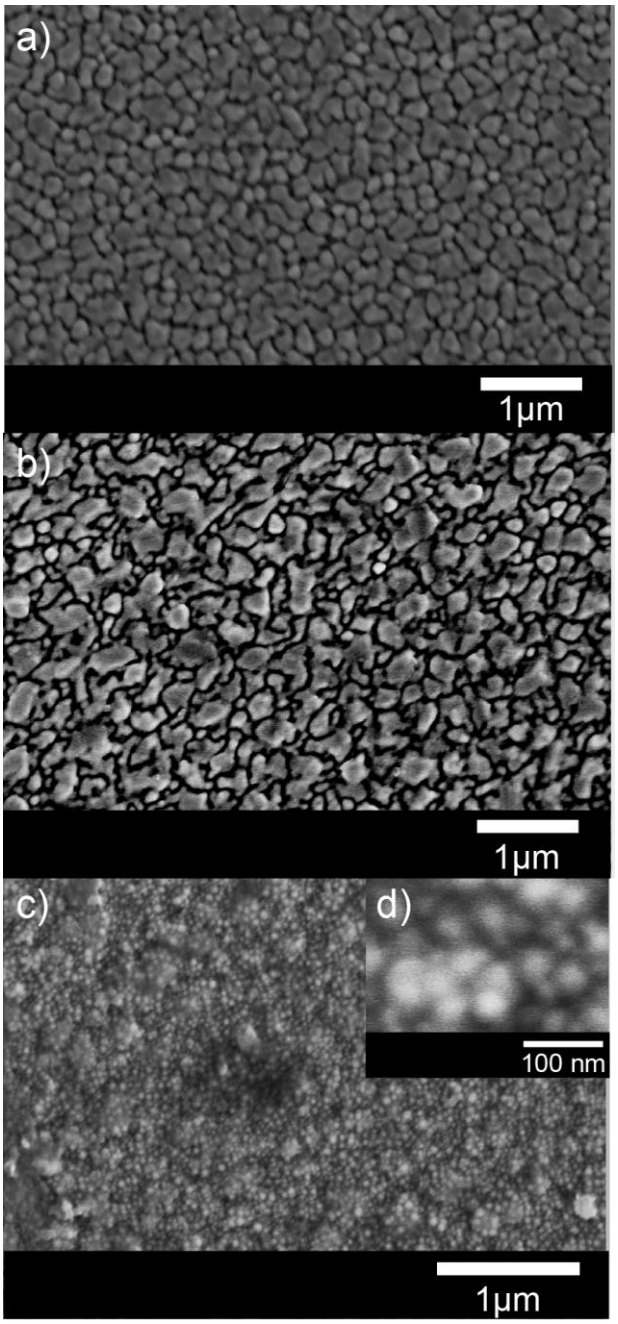

Figure 3: SEM images showing a) the Cu film b) ZrO_2 film c) Cu – ZrO_2 films grown *via* AACVD at 430 ^oC from a methanol solutions of [$Zr(acac)_4$] and [$Cu(NO_3)_2.3H_2O$].

Optical spectra from the ultraviolet to the near infrared region are shown in Figure 4. As expected, the Cu film showed metallic properties with low transmittance and high reflectivity in the near IR region. Transmittance in the visible region was also low at less than ca. 20%. The ZrO_2 film showed the typical high transmittance values in the visible (ca. 80%) and near IR (ca. 75%) regions. Reflectance for the ZrO_2 film was at ca. 20% across the whole spectrum analysed. In the near IR region the transmittance was between that of the Cu and the ZrO_2 film at ca. 30%. Reflectance in the IR region

was generally around 40% but between 600-700 nm there is a peak, which explains the brown/copper appearance of the film.

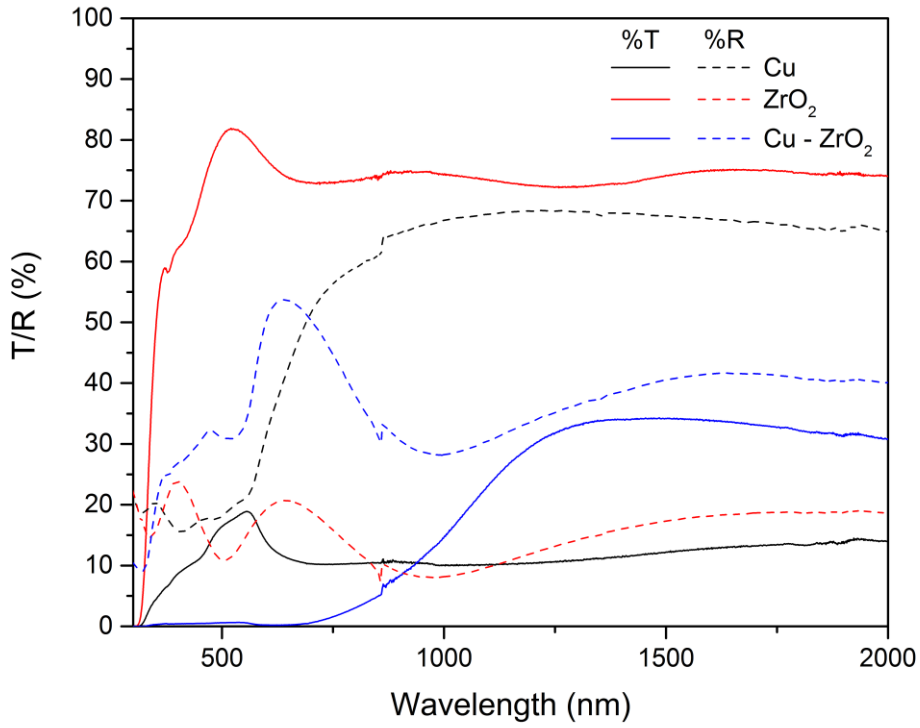

Figure 4: UV-Vis spectroscopy data for the Cu, ZrO_2 and Cu – ZrO_2 grown from [$Cu(NO_3)_2.3H_2O$], [$Zr(acac)_4$] and a mixture of the two for the composite film in a methanol solution *via* AACVD. The Cu film showed metallic properties as expected with low transmittance and high reflectance in the visible and near IR region. The ZrO_2 film was highly transparent in the visible and near IR region. Reflectance was roughly between 10 and 20% across the wavelengths measured. The Cu – ZrO_2 composite film is generally reflective in the visible region but transparent (35%) in the near IR.

The antibacterial activity of the AACVD deposited Cu, ZrO_2 and Cu – ZrO_2 films were tested against the Gram-negative bacterium *E. coli* and the Gram-positive bacterium *S. aureus* was determined (Figure 5). Initially samples were incubated with bacteria at 37 ^oC for 24 hours to determine if they had any antibacterial activity. The results show that both Cu and Cu-ZrO_2 composite film did indeed have antibacterial activity against both *E.coli* and *S.aureus*. As expected the pure ZrO_2 films showed no activity under the tested conditions.

Against *E. coli*, a 1.5 $\log_{10}$ and a 1.0 $\log_{10}$ reduction in the viable bacteria count of bacteria was recorded after 15 minutes of exposure to the Cu and Cu-ZrO_2 films

respectively. When the exposure time was increased to 20 minutes there was a significantly higher reduction in the number of viable *E. coli* recovered ($P < 0.01$) from both the Cu and Cu-ZrO_2 films, with a 4 log_{10} and 4.5 log_{10} reduction observed respectively. When tested against S. *aureus*, both the Cu and Cu-ZrO_2 films showed similar antibacterial activity. Over the first 45 minutes there was approximately ca. 2-log_{10} reduction in the number of viable bacteria. However between 45 and 60 minutes there was a dramatic decrease in the number of viable *S. aureus* to a level below the detection limit.

The inactivation of bacteria in contact ('contact killing') with Cu and Cu containing surfaces, such as in the case here, is thought to be due to a number of factors.[18, 41, 42] Although the process is complex and not fully understood, it is thought that Cu ions released into the surrounding solution from the antibacterial surfaces result in initial bacterial membrane damage which then causes an influx of Cu ions into cell.[41] The high intracellular Cu ion levels prove toxic to bacteria, resulting in cell death.

The results presented in this paper are comparable to previously reported antibacterial activity of Cu samples.[17, 42-44] The similar activity of the Cu – ZrO_2 film to the Cu film is attributed to the Cu rich surface of the composite film as shown from XPS analysis (Figure 2). Moreover, the Cu-ZrO_2 composite film is more mechanically robust compared to the Cu film thus making it more suitable for applications in medical applications.

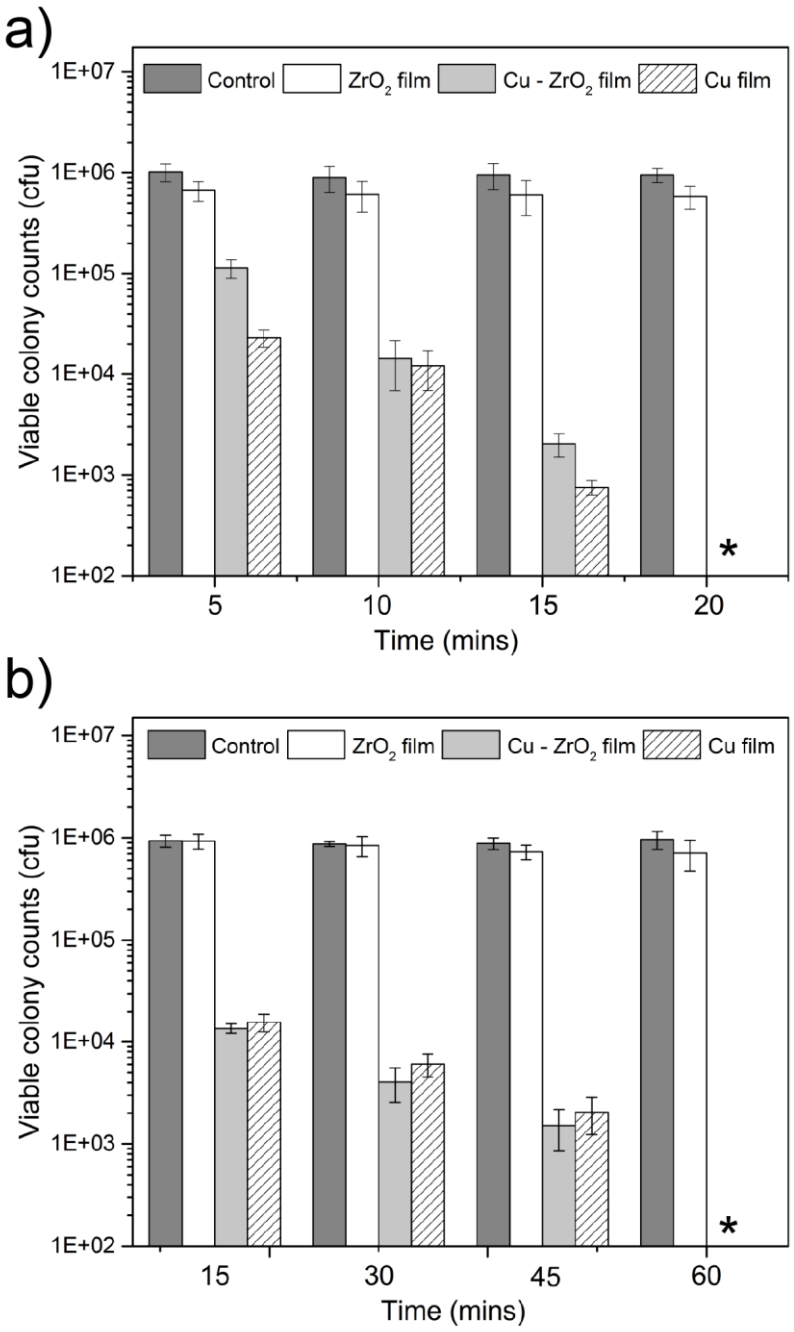

Figure 5: The viable counts of bacteria after incubation on Cu, ZrO_2 and Cu – ZrO_2 for a) *E. coli* and b) *S. aureus* under darkness. The Cu and the Cu – ZrO_2 films were able to reduce the bacterial numbers to below the limits of detection after 20 and 60 minutes for the *E. coli* and *S. aureus* respectively. The * indicates that the bacterial counts were below the detection limit of 100 cfu.

Conclusion

In summary, the composite Cu-ZrO_2 film grown from the AACVD reaction of $Cu(NO_3)_2.3H_2O$ and $Zr(acac)_2$ in methanol at 430 ^oC showed potential as a antibacterial coating for orthopedic implants. This is due mainly to:

- Antibacterial properties of the Cu component of the composite that showed high activity against *E. coli* and *S. aureus*.
- The biocompatibility and material toughness of the ZrO_2 constituent.
- High robustness to mechanical damage compared to the pure Cu

The film was able to cause a very significant reduction in bacterial numbers, giving 5 log_{10} kills of *E. coli* and 4 log_{10} *S. aureus* within 20 and 60 minutes respectively. This compares well with the pure copper film that was tested in this study, as well as with literature reports. [18, 41, 42]

XRD analysis showed evidence for the presence of two separate phases in the composite film, while XPS studies showed copper rich nature of the film surface, which is advantageous for antibacterial applications.

Acknowledgements

The authors would like to thank Dr. Iman A. Hassan for useful discussions and assistance with antibacterial analysis. Dr. Steve Firth and Dr. Tom Gregory are also thanked for SEM assistance. We are grateful to King Abdulaziz City for Science and Technology (KACST), Saudi Arabia for the provision of a PhD studentship to A.M.A and for financial support from the Saudi Cultural Bureau in London.

References

1. R. R. Roberts, I. R Douglas Scott, B. Hota, L. M. Kampe, F. Abbasi, S. Schabowski, I. Ahmad, G. G. Ciavarella, R. Cordell and S. L. Solomon, *Medical care*, 2010, **48**, 1026-1035.
2. G. Ducel, J. Fabry and L. Nicolle, *Prevention of hospital acquired infections: a practical guide*, 2002.
3. M. W. Climo, D. S. Yokoe, D. K. Warren, T. M. Perl, M. Bolon, L. A. Herwaldt, R. A. Weinstein, K. A. Sepkowitz, J. A. Jernigan and K. Sanogo, *N. Engl. J. Med.*, 2013, **368**, 533-542.
4. K. Page, R. G. Palgrave, I. P. Parkin, M. Wilson, S. L. P. Savin and A. V. Chadwick, *J. Mater. Chem.*, 2007, **17**, 95-104.
5. S. Noimark, J. Weiner, N. Noor, E. Allan, C. K. Williams, M. S. P. Shaffer and I. P. Parkin, *Adv. Funct. Mater.*, 2015, **25**, 1367-1373.
6. S. Perni, P. Prokopovich, J. Pratten, I. P. Parkin and M. Wilson, *Photochem. Photobiol. Sci.*, 2011, **10**, 712-720.
7. C. W. Dunnill, Z. Ansari, A. Kafizas, S. Perni, D. J. Morgan, M. Wilson and I. P. Parkin, *J. Mater. Chem.*, 2011, **21**, 11854-11861.
8. S. Perni, C. Piccirillo, A. Kafizas, M. Uppal, J. Pratten, M. Wilson and I. P. Parkin, *J. Cluster Sci.*, 2010, **21**, 427-438.
9. L. Zhao, P. K. Chu, Y. Zhang and Z. Wu, *Journal of Biomedical Materials Research Part B: Applied Biomaterials*, 2009, **91B**, 470-480.
10. E. M. Hetrick and M. H. Schoenfisch, *Chem. Soc. Rev.*, 2006, **35**, 780-789.
11. R. O. Darouiche, *N. Engl. J. Med.*, 2004, **350**, 1422-1429.
12. J. M. Schierholz, H. Steinhauser, A. F. E. Rump, R. Berkels and G. Pulverer, *Biomaterials*, 1997, **18**, 839-844.
13. S. Rossi, A. O. Azghani and A. Omri, *J. Antimicrob. Chemother.*, 2004, **54**, 1013-1018.
14. Y. Z. Wan, G. Y. Xiong, H. Liang, S. Raman, F. He and Y. Huang, *Appl. Surf. Sci.*, 2007, **253**, 9426-9429.
15. Y. Z. Wan, S. Raman, F. He and Y. Huang, *Vacuum*, 2007, **81**, 1114-1118.
16. H.-L. Huang, Y.-Y. Chang, J.-C. Weng, Y.-C. Chen, C.-H. Lai and T.-M. Shieh, *Thin Solid Films*, 2013, **528**, 151-156.
17. I. A. Hassan, I. P. Parkin, S. P. Nair and C. J. Carmalt, *Journal of Materials Chemistry B*, 2014, **2**, 2855-2860.
18. J. P. Ruparelia, A. K. Chatterjee, S. P. Duttagupta and S. Mukherji, *Acta Biomaterialia*, 2008, **4**, 707-716.
19. C. E. Santo, P. V. Morais and G. Grass, *Appl. Environ. Microbiol.*, 2010, **76**, 1341-1348.
20. J. Ramyadevi, K. Jeyasubramanian, A. Marikani, G. Rajakumar and A. A. Rahuman, *Mater. Lett.*, 2012, **71**, 114-116.
21. R. Jayakumar, R. Ramachandran, P. T. S. Kumar, V. V. Divyarani, S. Srinivasan, K. P. Chennazhi, H. Tamura and S. V. Nair, *Int. J. Biol. Macromol.*, 2011, **49**, 274-280.
22. C. E. Knapp and C. J. Carmalt, *Chem. Soc. Rev.*, 2016.
23. X. Hou and K. L. Choy, *Chem. Vap. Deposition*, 2006, **12**, 583-596.
24. P. Marchand, I. A. Hassan, I. P. Parkin and C. J. Carmalt, *Dalton Trans.*, 2013, **42**, 9406-9422.
25. S. Sathasivam, R. R. Arnepalli, B. Kumar, K. K. Singh, R. J. Visser, C. S. Blackman and C. J. Carmalt, *Chem. Mater.*, 2014, **26**, 4419-4424.

26. S. M. Bawaked, S. Sathasivam, D. S. Bhachu, N. Chadwick, A. Y. Obaid, S. Al-Thabaiti, S. N. Basahel, C. J. Carmalt and I. P. Parkin, *J. Mater. Chem. A*, 2014, **2**, 12849-12856.
27. D. S. Bhachu, S. Sathasivam, G. Sankar, D. O. Scanlon, G. Cibin, C. J. Carmalt, I. P. Parkin, G. W. Watson, S. M. Bawaked, A. Y. Obaid, S. Al-Thabaiti and S. N. Basahel, *Adv. Funct. Mater.*, 2014, **24**, 5075-5085.
28. S. Sathasivam, D. S. Bhachu, Y. Lu, N. Chadwick, S. A. Althabaiti, A. O. Alyoubi, S. N. Basahel, C. J. Carmalt and I. P. Parkin, *Scientific reports*, 2015, **5**.
29. S. Sathasivam, R. R. Arnepalli, K. K. Singh, R. J. Visser, C. S. Blackman and C. J. Carmalt, *RSC Advances*, 2015, **5**, 11812-11817.
30. S. Ponja, S. Sathasivam, N. Chadwick, A. Kafizas, S. M. Bawaked, A. Y. Obaid, S. Al-Thabaiti, S. N. Basahel, I. P. Parkin and C. J. Carmalt, *J. Mater. Chem. A*, 2013, **1**, 6271-6278.
31. I. A. Hassan, A. Ratnasothy, D. S. Bhachu, S. Sathasivam and C. J. Carmalt, *Aust. J. Chem.*, 2013, **66**, 1274-1280.
32. D. Prakashbabu, R. Hari Krishna, B. M. Nagabhushana, H. Nagabhushana, C. Shivakumara, R. P. S. Chakradar, H. B. Ramalingam, S. C. Sharma and R. Chandramohan, *Spectrochimica Acta Part A: Molecular and Biomolecular Spectroscopy*, 2014, **122**, 216-222.
33. A. M. Alotaibi, S. Sathasivam and I. P. Parkin, *RSC Advances*, 2015, **5**, 67944-67950.
34. P. Keil, D. Lützenkirchen-Hecht and R. Frahm.
35. H. H. Strehblow and B. Titze, *Electrochim. Acta*, 1980, **25**, 839-850.
36. H. D. Speckmann, S. Haupt and H. H. Strehblow, *Surf. Interface Anal.*, 1988, **11**, 148-155.
37. G. K. P. Ramanandan, G. Ramakrishnan and P. C. M. Planken, *J. Appl. Phys.*, 2012, **111**, 123517.
38. S. Suzuki, Y. Ishikawa, M. Isshiki and Y. Waseda, *Mater. Trans. JIM*, 1997, **38**, 1004-1009.
39. M. C. Biesinger, L. W. M. Lau, A. R. Gerson and R. S. C. Smart, *Appl. Surf. Sci.*, 2010, **257**, 887-898.
40. G. Deroubaix and P. Marcus, *Surf. Interface Anal.*, 1992, **18**, 39-46.
41. G. Grass, C. Rensing and M. Solioz, *Appl. Environ. Microbiol.*, 2011, **77**, 1541-1547.
42. S. L. Warnes and C. W. Keevil, *Appl. Environ. Microbiol.*, 2011, **77**, 6049-6059.
43. S. L. Warnes, V. Caves and C. W. Keevil, *Environmental microbiology*, 2012, **14**, 1730-1743.
44. S. W. J. Gould, M. D. Fielder, A. F. Kelly, M. Morgan, J. Kenny and D. P. Naughton, *Annals of microbiology*, 2009, **59**, 151-156.

Supporting Information

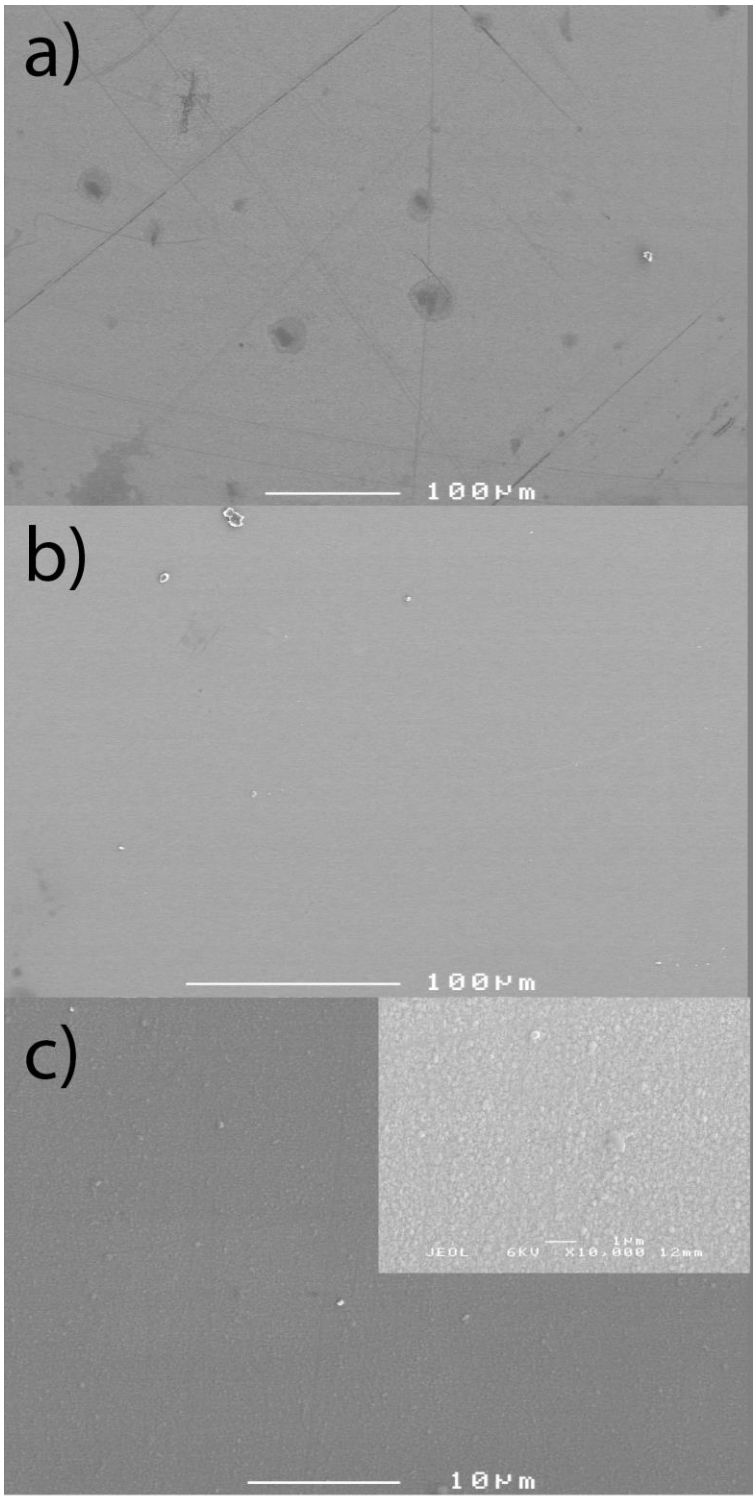

Figure 6: SEMs of the a) Cu, b) ZrO_2 and c) Cu-ZrO_2 (magnified image inset) films after light abrasion test using a metal spatula. The Cu film was readily scratched by whereas the ZrO_2 and the composite Cu-ZrO_2 were more resistant to damage. The low magnification SEM images also the films free of cracks and pinholes.

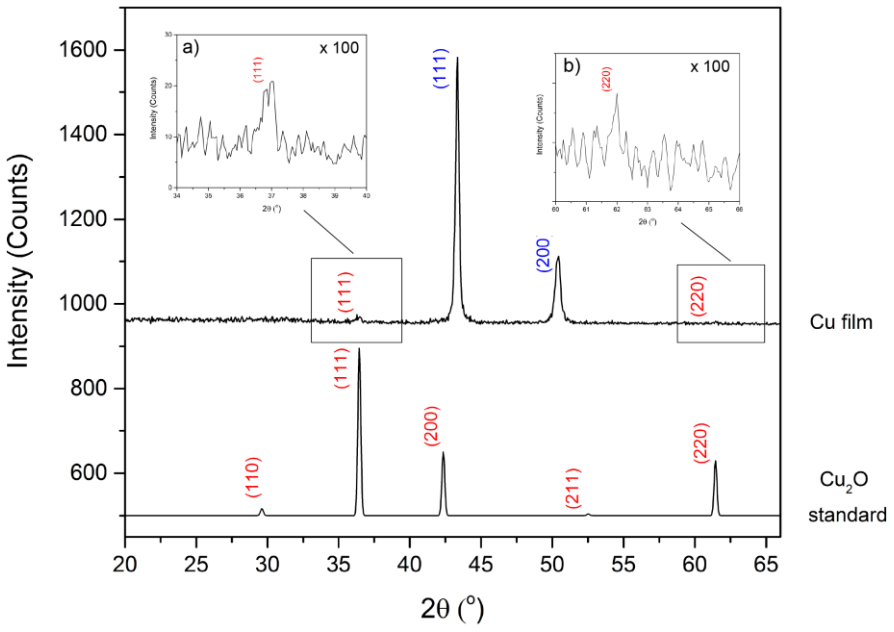

Figure 1 (SI): The XRD pattern for the Cu film grown *via* AACVD. When the 34-40º and 60-65º 2θ regions are magnified peaks matching to the (111) and (220) reflections of Cu_2O (standard pattern also shown) are evident. Note (hkl) values in red are for Cu_2O and blue for Cu metal.

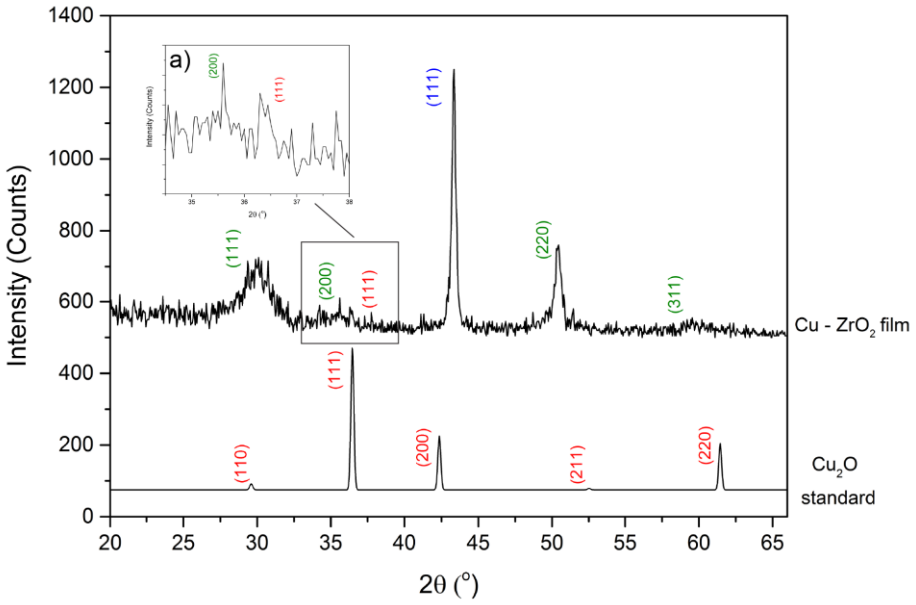

Figure 2 (SI): The XRD pattern for the Cu – ZrO_2 film grown *via* AACVD. When the 34-40º 2θ region magnified peaks matching to the (111) Cu_2O (standard pattern also shown) is evident. Note (hkl) values in red are for Cu_2O, green for ZrO_2 and blue for Cu metal.

Table 1: Estimated crystallite size calculated from XRD data using the Debye – Scherrer formula.

	hkl	Bragg Angle 2θ/°	θB/rad	cos(θB)	βcos(θB)	Diameter/nm
Cu	111	43.3	0.3782	0.9293	0.0051	27
	200	50.4	0.4397	0.9049	0.0069	20
ZrO_2	111	30.4	0.2649	0.9651	0.0169	8
	200	35.2	0.3068	0.9533	0.0142	10
	220	50.6	0.4413	0.9042	0.0236	6
Cu-ZrO_2	111 (ZrO_2)	30.0	0.2614	0.9660	0.0348	4
	111 (Cu)	43.3	0.3782	0.9293	0.0057	24
	220 (ZrO_2)	50.4	0.4399	0.9048	0.0092	15

Table 2: XPS elemental analysis showing peak area and corrected peak area for a) Cu (0) / Cu (I) 2p b) Cu (II) 2p and Zr (IV) 2p. c) Shows the Cu to Zr and Cu (0) / Cu(I) to Cu (II) ratios.

a)

	Cu (0) / Cu (I)
2p3/2 area	237752
2p1/2 area	118876
2p area	356627
R.S.F	6.3
Corrected 2p area	56608

b)

	Cu (II)
2p3/2 area	39658
2p1/2 area	19829
2p area	59488
Shake-up satellite peak area	13398
R.S.F	6.3
Corrected area	11569

c)

	Zr (IV)
3d5/2 area	38108
3d3/2 area	25418
3d area	63526
R.S.F	2.1
Corrected 2p area	30250

d)

Cu : Zr	2.3
Cu (0)/Cu (I) : Cu (II)	4.9

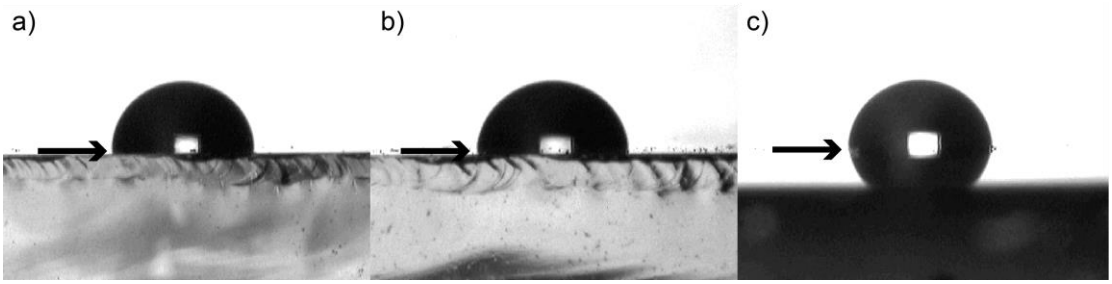

Figure 3 (SI): The water contact angle on the surface of a) Cu, b) ZrO_2 and c) Cu - ZrO_2 films grown *via* AACVD at 430 ^oC. The arrows show the contact line.

Wettability studies on the films determined *via* water contact angle measurements show that the contact angle is similar (ca. 95^o) for all the AACVD prepared films. Thus eliminating the contact between the bacteria solution and the film as a variable.